A Numerical Study of Chemical Reaction in a Nanofluid Flow Due to Rotating Disk in the Presence of Magnetic Field

Muhammad Ramzan
King Mongkut's University of Technology Thonburi
Poom Kumam (poom.kum@kmutt.ac.th)
China Medical University Hospital
Kottakkaran Sooppy Nisar
Prince Sattam Bin Abdulaziz University
Ilyas Khan
Majmaah University
Wasim Jamshed
Capital University of Science and technology (CUST) Islamabad

Research Article

Keywords: Nanofluid, MHD, Rotating disk, Chemical reaction, Heat source

Posted Date: March 1st, 2021

DOI: https://doi.org/10.21203/rs.3.rs-242270/v1

A Numerical Study of Chemical reaction in a Nanofluid flow due to rotating disk in the presence of Magnetic Field

Muhammad Ramzan[1], Poom Kumam[*,1,2], Kottakkaran Sooppy Nisar[3,] Ilyas Khan[4], Wasim Jamshed[5]

[1]Center of Excellence in Theoretical and Computational Science (TaCS-CoE) & KMUTT Fixed Point Research Laboratory, Room SCL 802 Fixed Point Laboratory, Science Laboratory Building, Departments of Mathematics, Faculty of Science, King Mongkut's University of Technology Thonburi (KMUTT), 126 Pracha-Uthit Road, Bang Mod, Thrung Khru, Bangkok 10140, Thailand

[2]Department of Medical Research, China Medical University Hospital, China Medical University, Taichung 40402, Taiwan

[3] Department of Mathematics, College of Arts and Sciences, Wadi Aldawaser, 11991, Prince Sattam bin Abdulaziz University, Saudi Arabia

[4]Department of Mathematics, College of Science Al-Zulfi, Majmaah University, Al-Majmaah 11952, Saudi Arabia

[5]Department of Mathematics, Capital University of Science and Technology (CUST), 44000, Islamabad, Pakistan

*Corresponding author: Poom Kumam (e-mail: poom.kum@kmutt.ac.th).

Abstract:

In this paper, a numerical study of MHD steady flow due to the rotating disk with chemical reaction was explored. Effect of different parameters such as Schmidt number, chemical reaction parameter, Prandtl number, Suction parameter, heat absorption/generation parameter, Nano-particle concentration, Reynold number, Magnetic parameter, skin friction, shear stress, temperature distribution, Nusselt number, mass transfer rate, radial velocity, axial velocity, and tangential velocity was analyzed and discussed. For the simplification of non-linear partial differential equations (PDEs) into the nonlinear ordinary differential equation (ODEs), the method of Similarity transformation was employed, and the resulting partial differential

equation was solved by using finite difference method through MATLAB programming. This work's remarkable finding is that with the expansion of nanoparticle concentration radial velocity, tangential velocity and temperature of the fluid was enhanced but reverse reaction for axial velocity. Furthermore, the present results are found to be in excellent agreement with previously published work.

Key words: Nanofluid, MHD, Rotating disk, Chemical reaction, Heat source.

1. Introduction

The flow problem due to rotating disk is much interest of scientist over the last few years because of its vast application in industrial and engineering process such as spin coating, centrifugal pumps, rotor-stator system, electronic device, turbo machinery and multi power distributor manipulative, etc. Nanofluid described as nanoparticles embedded inside the fluid with size less than 100nm. Nanofluid has wide applications in cooling towers, in cancer patient detection of drugs, the efficiency of the hybrid powered engine, and transportation. Due to rotating disk with heat flux conditions and irregular heat source, the nonlinear radiated MHD flow of nanofluids was studied by Mahanthesh *et al.* [1]. He used the Runge – Kutta Fehlberg method to find the solution of their problem numerically and also discuss the different results of velocities and temperature graphically. By using partial slip conditions over a rotating disk the magnetohydrodynamic flow of Cu-Water nanofluid was investigated by Hayat *et al.* [2] and the Homotopy analysis technique was hired to find the numerical results of their heat and flow transfer model and also detected that by increasing the nanoparticle volume fraction the heat transfer rate was increased. Radial and azimuthal velocities were reduced with the enhancement of velocity slip parameters, while for larger values of slip parameters the temperature of the fluid is decreased. Yin *et al.* [3] was analyzed that with the occurrence of a uniform stretching rate in the radial direction, the heat and

flow transfer of a nanofluid over the disk which is rotating. To find the solution of their mathematical model numerically he engaged the Homotopy analysis method (HAM) and his research work shows that the velocity in an axial and radial direction the coefficient of skin friction and local Nusselt number was enhanced with the increasing of stretching strength parameter, while the velocity in tangential direction and thickness of thermal boundary layer were decreased. In the presence of slip conditions over a disk which is rotating, the magnetohydrodynamic flow of nanofluid was explored by Hayat *et al.* [4] used by the bvp4c techniques. During his research work, he performed the computation for Sherwood number and Nusselt Number and also checked the impact of a different parameter over the temperature, concentration, and velocity profile of the fluid. For low magnetic Reynolds number the induced magnetic field is neglected. The properties of a magnetohydrodynamic over the slip flow with variable thickness was initiated by Imtiaz *et al.* [5] applied the homotopy analysis technique for the solution of their problem and obtained the convergent series solution of their model. His conclusion shows that over thickness coefficient over a thickness of a rotating disk the effect of radial and axial velocities is reverse and also for Hertman number and drag force has a direct relationship with each other. In the presence of variable thickness, the slip flow and entropy generation in Magnetohydrodynamic on a rotating porous disk was presented by Rashidi *et al.* [6]. To obtain the numerical solution of their model von Karman approach was employed and also discussed the impact of different parameters named relative temperature difference, suction injection parameter and slip effect for a different profile of axial tangential and radial velocities and temperature, average Bejan Number, and average entropy generation. By the impact of partial slip, the MHD nanofluid over disk which is rotating through the use of the Buongiorno model was proposed by Mustafa *et al.* [7] and with the applying of shooting technique, he solved the given model numerically. His research analysis shows that the velocity distribution

and magnetic parameter are inverse to each other also over a momentum transport the velocity slip impact are opposite but axial velocity is negative due to the Brownian motion of the fluid in a disk and also the thermophoretic force increased the thermal and concentration boundary layer thickness. Over a rotating disk the heat transfer and nanofluid flow with the implementation of spectral Chebyshev collection numerical integration scheme was perceived Turkyilmazoglu [8] also in the research work he made a comparison between cooling properties and shear stress of the nanofluid. For various nanoparticle volume fraction values, the properties of heat transfer and shear stress as well as flow and temperature field were assessed, and found that with the increment of Cu-nanofluid the heat transfer rate is enhanced. Over a porous medium disk, the heat transfer and Marangoini boundary layer flow of copper-water nanofluid were demonstrated by Lin *et al.* [9] with the impose of generalized Karman transformation to convert the PDEs into the ODEs and solved these ordinary differential equations by the shooting technique and homotopy analysis method (HAM) and then he presents the impact of different parameter Marangoini parameter, solid volume fraction and permeability parameter over the temperature and velocity of the fluid graphically. For the cooling process over a disk which is inclined to rotate the numerical investigation of a nanofluid was produced by Sheikholeslami *et al.* [10] and fourth-order Runge – Kutta method was utilized for the numerical solution of their model and also found that latent heat has reversed relationship with the normalized thickness but for direct relation for Schmidt number, Brownian motion and thermophoretic parameter. Also, the thermophoretic parameter and Schmidt number is an increasing effect over a Brownian motion parameter. On a rotating disk which is porous and rough the mass and heat transfer of flow was expressed by Turkyilmazoglu and Senel [11]. To obtain their results numerically the fourth order Runge – Kutta method was employed and determined that the suction and injection are in opposite behavior and for the mass and

heat transfer, the surface roughness and slip are decreased. Also, in the radial direction with the increment of slip parameter, the radial shear stress is reduced. Due to a rotating disk the hydromagnetic flow with radiation impact is perceived by Devi and Devi [12]. For the numerical solution of their problem Runge – Kutta method with shooting technique was used and also discuss the behavior of magnetic and radiation parameter on their problem. The slip flow and magnetohydrodynamic over a rotating disk which is porous through variable thickness in the existence of thermal radiation was done by Osalusi [13] with the help of shooting techniques. Due to the rotating disk the analytical modeling for heat transfer of the couple stress and unsteady MHD flow is pointed out by Khan *et al.* [14] and also Runge – Kutta method with shooting technique was hired for the solution of their model numerically and also explain the variation of physical parameters over the pressure, temperature and velocity profile of the fluid. In the occurrence of heat transfer over the rotating disk with MHD and slip flow was examined by Arikoglu and Ozkol [15] with the applying of the differential transform method, the result of their model is obtained and realized that the velocity of the fluid in radial, axial and tangential direction should be decreased with magnetic flux and slip flow. Nadeem et al. [16] used optimal homotopy asymptotic method (OHAM) to find the exact solution of 2nd Grade nanofluid over a rotating vertical cone with nanoparticles i.e Brownian motion and thermophoresis. They used the Buongiorno nanofluid model and detected that for growing values of N and s, the rate of heat transfer and Sherwood number shows a rising behavior. Hafeez et al. [17] investigated the 3D Oldroyd-B nanofluid over a rotating disk under the effects of Stagnation point flow via BVP Midrich technique. They concluded that for higher values disk convection parameter and radiative heat flux demonstrate a rising behavior of temperature distribution of the Oldroyed-B nanofluid. Finally, Abbasi et al. [18] examined the non-Newtonian viscoelastic nanofluid over a rotating disk with heat source. They utilized

the Keller box scheme for the numerical results and discussed the effects of different physical parameters effecting flow and heat transfer. They found the diffusion of thermophoresis increases both the temperature and the concentration profiles. Recent additions considering nanofluids with heat and mass transfer in various physical situations are given by [19-31]

In aforementioned studies and a comprehensive literature review, it is disclosed that no such study has been carried out and is currently available to examine the heat transfer and magnetically driven nanofluid flow over the rotating disk in the occurrence of chemical reaction was examined. The partial differential equation of the model can be converted into an ordinary differential equation with the help of similarity transformation and solved these ordinary differential equations by using finite difference method. Then the effect of different parameters is analyzed and discussed in following sections.

2. Description of Physical Model

Consider a porous rotating disk the steady, axially symmetric laminar flow of nanofluid with heat generation/ absorption was explored here. Over the surface of rotating disk, the uniform magnetic field is applied perpendicularly.

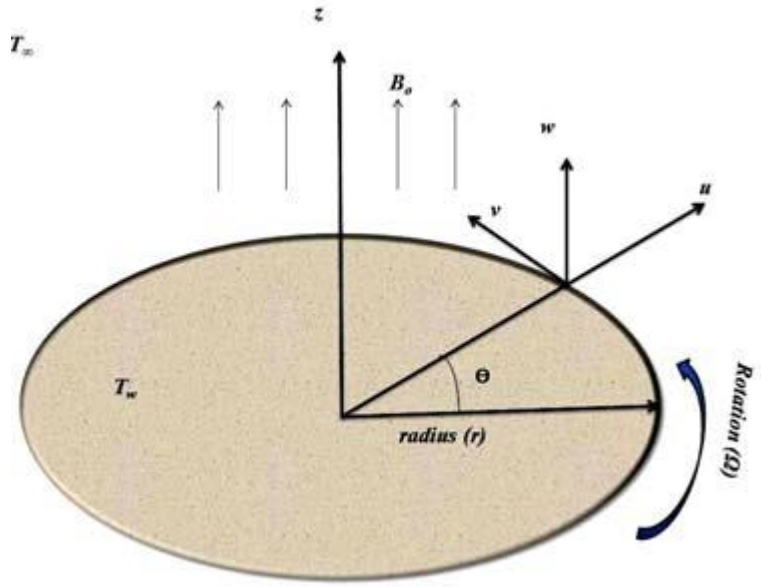

Figure (A)

The z-axis is taken perpendicular into the surface of rotating disk while in r, Θ and z direction the velocities are denoted by the u, v and w in cylindrical coordinate system. T_w, Is the temperature of the disk and ambient temperature of the fluid is T_∞. Fig (A) describe the physical model of the problem

Under the above assumptions the governing equation for the present flow and heat transfer model are given below

2.1 Governing Equations

$$\frac{\partial u}{\partial r}+\frac{u}{r}+\frac{\partial w}{\partial z}=0 \tag{1}$$

$$u\frac{\partial u}{\partial r}+w\frac{\partial u}{\partial z}-\frac{v^2}{r}\frac{1}{\rho_{nf}}\frac{\partial p}{\partial r}=v_{nf}\left(\frac{\partial^2 u}{\partial r^2}+\frac{\partial^2 u}{\partial z^2}\right)-\frac{\sigma B_o u}{\rho_{nf}} \tag{2}$$

$$u\frac{\partial v}{\partial r}+w\frac{\partial v}{\partial z}+\frac{uv}{r}=v_{nf}\left(\frac{\partial^2 v}{\partial r^2}+\frac{\partial^2 v}{\partial z^2}\right)-\frac{\sigma B_o u}{\rho_{nf}} \tag{3}$$

$$u\frac{\partial w}{\partial r}+w\frac{\partial w}{\partial z}\frac{1}{\rho_{nf}}\frac{\partial p}{\partial r}=v_{nf}\left(\frac{\partial^2 w}{\partial r^2}+\frac{\partial^2 w}{\partial z^2}\right) \tag{4}$$

$$u\frac{\partial T}{\partial r}+w\frac{\partial T}{\partial z}=\frac{k_{nf}}{\left(\rho C_p\right)_{nf}}\left(\frac{\partial^2 T}{\partial r^2}+\frac{\partial^2 T}{\partial z^2}\right)+Q_0 \tag{5}$$

$$u\frac{\partial c}{\partial r}+w\frac{\partial c}{\partial r}=D\nabla^2 c-k(c-c_\infty) \tag{6}$$

Where Q_0 is used for the heat generation/absorption and properties of the nanofluid is denoted by the subscript "*nf* ".

2.2 Boundary Conditions:

$$\left.\begin{array}{l} u=0, v=r\Omega\ , w=w_0, T=T_w\ \ at\ \ z=0, \\ u\to 0\ ,\ v\to 0\ \ , P\to P_\infty,\ \ T\to T_\infty\ \ ,\ at\ \ z\to\infty \end{array}\right\} \tag{7}$$

2.3 Nanofluid Properties are:

$$\left.\begin{array}{l} \rho_{nf}=\phi\rho_p+(1-\phi)\rho_f \\ (\rho C_p)_{nf}=\phi(\rho C_p)_p+(1-\phi)(\rho C_p)_f \end{array}\right\} \tag{8}$$

Around the nanoparticle to analyze the role of nanoparticle concentration, nano thermal layer, and nanoparticle size designed by the fluid and maintain the theoretical validity of the nanofluid with thermo physical characteristics, suitable model for effective thermal conductivity and efficient viscosity. The Nanofluid viscosity is specified through

$$\mu_{nf}=\frac{\mu_f}{1-34.870(d_p/d_f)^{-0.30}\phi^{1.030}} \tag{9}$$

$$d_f=\left[\frac{6M_0}{\rho_{f_0}\pi N}\right]^{\frac{1}{3}}0.1$$

Now d_f represents the diameter of molecule base fluid, M_0 stands for base fluid molecular mass, then Avogadro's number is denoted by N (N= 6.023e+0233). At a reference temperature the base fluid mass density is express by the ρ_{f_0} . For water ρ_{f_0}

=998.2 and M_0=18.023e-0333. The effective nanofluids thermal conductivity is defined as below.

$$k_{nf} = \left[\frac{k_{pe} + 2k_f + 2(k_{pe} - k_f)(1-\beta^3)\phi}{k_{pe} + 2k_f - 2(k_{pe} - k_f)(1+\beta^3)\phi} \right] k_f \tag{10}$$

$$k_{pe} = \left[\frac{2(1-\gamma) + (1-\beta)^3(1+2\gamma)}{-2(1-\gamma) + (1+\beta)^3(1+2\gamma)} \right] k_f \tag{11}$$

$$\gamma = \frac{k_{layer}}{k_p} \text{ and } \beta = \frac{h}{r_p}$$

Where base fluid thermal conductivity is designed by k_f , r_p is used for radius of Nano atom, for Nano atom thermal conductivity is denoted by k_p and diameter is expressed by d_p, around the nanoparticle the thickness of nano layer is described by h which is formed by the fluid and Nano layer the thermal conductivity is described by k_{layer}. It was noticed from experimental results k_{layer}=100k_f. Dimensionless variable is introduced for the simplification of equation (1-6) by using boundary condition (7):

$$\left.\begin{aligned} &\eta = (\frac{\Omega}{\upsilon_f})^{\frac{1}{2}} z, u = \Omega r F(\eta), v = \Omega r G(\eta), w = (\upsilon_f \Omega)^{\frac{1}{2}} H(\eta), P - P_\infty = 2\Omega\mu_f p(\eta) \\ &\theta(\eta) = \frac{T - T_\infty}{(T_w - T_\infty)}, \xi(\eta) = \frac{c - c_w}{c_w - c_\infty}, Q = \frac{Q_0}{\Omega(T_w - T_\infty)} \end{aligned}\right\} \tag{12}$$

With the help of thermo-physical properties of nanofluid (7-11) and dimensionless variable (12), the partial differential equation (2-6) can be transformed into ordinary differential

$$F' + 2F(\eta) = 0 \tag{13}$$

$$\frac{1}{\left[1 - \phi + \phi\rho_s / \rho_f\right]} \left[\frac{1}{1 - 34.87(d_p / d_f)^{-0.3} \phi^{1.03}} \right] F'' = HF' + F^2 - G^2 + MF \tag{14}$$

$$\frac{1}{\left[1 - \phi + \phi\rho_s / \rho_f\right]} \left[\frac{1}{1 - 34.87(d_p / d_f)^{-0.3} \phi^{1.03}} \right] G'' = HG' + 2FG + MG \tag{15}$$

$$\frac{1}{pr}\frac{k_{nf}/k_f}{(\rho c_p)_{nf}/(\rho c_p)_f}\theta''-H\theta'+Q=0 \tag{16}$$

$$d_1.Sc.\xi'(\eta)H(\eta)=\xi''(\eta)-\gamma.\frac{1}{R}d_1\xi(\eta) \tag{17}$$

Boundary conditions are given:

$$\left.\begin{array}{l} F(0)=0, G(0)=0, H(0)=W_s, \theta(0)=1 \\ F(\infty)\to 0, G(\infty)\to 0, \theta(\infty)\to 0 \end{array}\right\} \tag{18}$$

Here F, G, H and Θ are a dimensionless parameter for the temperature and velocities of the fluid, the suction parameter is denoted by w_s, Magnetic parameter is symbolized by M, Prandtl number is indicated by p_r and η is dimensionless distance.

$$w_s=\frac{w_0}{\left(\upsilon_f\Omega\right)^{\frac{1}{2}}},\ M=\frac{\sigma B_o^2}{\Omega\rho_{nf}},\ p_r=\frac{\rho C_p\upsilon}{k_f},\ Sc=\frac{\upsilon_f}{D},\ \gamma=\frac{KL^2}{D},\ \frac{1}{R}=\frac{\upsilon}{L^2\Omega}$$

2.4 Physical Quantities:

The skin friction coefficient and heat transfer coefficient are given by

$$C_f=\frac{\sqrt{\tau_{rw}{}^2+\tau_{\phi w}^2}}{(r\Omega)^2\rho_f},\qquad Nu=\frac{q_w r}{(T_w-T_\infty)k_f}$$

Over the surface of a disk the radial and transversal shear stresses and heat flux is represented by $\tau_{\phi w}$, τ_{rw}, q_w respectively and defined as

$$\tau_{rw}=\left|(w_\phi+u_z)\mu_f\right|_{z=0},\quad \tau_{\phi w}=\left[(\frac{1}{r}w_\phi)+v_z)\mu_f\right]_{z=0},\quad q_w=-k_f(T)_{z=0}$$

Implementation of dimensionless parameters set in equation (12), another dimensionless mathematical interpretation for coefficient of skin friction and Nusselt number is given as

$$C_f\,\mathrm{Re}^{(\frac{-1}{2})}=\frac{\sqrt{F'(0)^2+G'(0)^2}}{1-34.87(d_p/d_f)^{-0.3}\phi^{1.030}},\ \mathrm{Nu}\,\mathrm{Re}^{(\frac{-1}{2})}=-\theta'(0)\frac{k_{nf}}{k_f}$$

$\mathrm{Re}=\Omega\frac{r^2}{\upsilon_f}$ is used for local Reynold number.

3. Numerical Analysis

The governing ODE's (14) - (17) being extremely non-linear are not easy to solve analytically. We obtain the numerical solution of these equations with help of finite difference technique based on numerical algorithms. This method is preferred over many other methods due to its fast convergence. This scheme is inherently stable and is second-order convergent.

$$F_{i-1}\left(2d+hH_i\right)+F_{i+1}(2d-hH_i)-F_i(4d+2h^2F_i+\frac{d_2}{d_3}M)+2h^2G_i=0 \tag{19}$$

$$G_{i-1}\left(2d+hH_i\right)+G_{i+1}(2d-hH_i)-G_i(4d+4h^2F_i+2h^2\frac{d_2}{d_3}M)+2h^2G_i=0 \tag{20}$$

$$\theta_{i-1}(2D+hH_i)+\theta_{i+1}(2D-hH_i)-4D\theta_i+2h^2Q=0 \tag{21}$$

$$\zeta_{i-1}\left(2+hd_1ScH_i\right)+\zeta_{i+1}\left(2-hd_1ScH_i\right)-\zeta_i\left(h+2h^2\frac{r}{\mathrm{Re}}d_1\right)=0 \tag{22}$$

3.1 Computational Procedure & Code Validation

The equations (14) – (17) are solved with the help of SOR method subject to the suitable boundary values given in equation (18). An iterative procedure is started for the solution vectors $f, g, \theta \text{ and } \zeta$ with the help of grid size h and ω (relaxation parameter), where kth iteration of these vectors performs the following steps:

I . In next approximations for the solution of equations (19) – (22) g^{k+1}, $\theta^{k+1}$and ζ^{k+1} are formed by successive over relaxation technique.

II. The value of f^{k+1} is determined with the help of Simpson's rule. Where g^{k+1}, $\theta^{k+1}$and ζ^{k+1} are used to find the value of $g, \theta \text{ and } \zeta$ in equations (19) – (22) to obtain the solution of equation (13).

III. The convergence obtained by comparing $g^{k+1}, \theta^{k+1}, \zeta^{k+1}$and f^{k+1} with $g^k, \theta^k, \zeta^k$and f^k correspondingly. If the criteria explained below is satisfied for consecutive four iterations then the procedure of iteration is stopped.

$Max\ (\|g^{k+1} - g^k\|_2, \|\theta^{k+1} - \theta^k\|_2, \|\zeta^{k+1} - \zeta^k\|_2, \|f^{k+1} - f^k\|_2 \quad < TOL_{iter}$

Here TOL_{iter} defined error tolerance.

3.2 Code Validation

The numerical validation was assessed and compared from the results of existing literature [32-37]. The comparison shown in Table 1, seems to be in strong accordance. However, the outcomes of present study are highly accurate.

Table 1: Comparitive variation of -$\theta'(0)$ with Prandtl number, on taking $\phi = 0$ and $Q = 0$.

P_r	[32]	[33]	[34]	[35]	[36]	[37]	***Present*** Results
0.72	0.8086	0.8086	0.80863135	0.80876122	0.80876181	0.80876181	0.80876181
1.0	1.0000	1.0000	1.00000000	1.00000000	1.00000000	1.00000000	1.00000000
3.0	1.9237	1.9236	1.92368259	1.92357431	1.92357420	1.92357420	1.92357420
7.0	3.0723	3.0723	3.07225021	3.07314679	3.07314651	3.07314651	3.07314651
10	3.7207	3.7006	3.72067390	3.72055436	3.72055429	3.72055429	3.72055429

4. Results and Discussions

The tabular and graphically representation of different parameters are discussed here, the Reynold number Re, chemical reaction parameter γ, Magnetic parameter M, Suction parameter Ws, Prandtl number P_r, heat absorption/generation parameter Q, Nano-particle concentration ϕ, Schmidt number Sc, skin friction C_f, shear stress $f''(\eta)$, temperature distribution $\theta'(\eta)$, Nusselt number Nu, mass transfer rate $\zeta'(\eta)$, radial velocity $f'(\eta)$, axial velocity $h'(\eta)$ tangential velocity $g'(\eta)$. From Table .2 which

describe the numerical values of different parameter such as Nano-particle, Magnetic field, Suction parameter for shear stress, Nusselt number and heat and mass transfer rate. We observed that heat and mass transfer rate are increased but shear stress and Nusselt Number are reduced with the increase of nanoparticle. Also, it was noticed that the shear stress is enhanced but heat transfer rate, Nusselt Number, and the mass transfer rate are diminished with the enhancement of the Magnetic field. Table 3 can be explained that the suction parameter has same effect over the shear stress, Nusselt Number and heat, and mass transfer rate, it means for higher values of suction parameter the values of all these parameters are decreased. For different values of the Prandtl Number, chemical reaction, and heat absorption parameter the variance of the heat transfer rate, Nusselt number, and mass transfer rate are presented in Table 3. It was shown that both the heat, and mass transfer rate are increased due to an increase in the Prandtl number values. Table can also explore that with the enhancement of chemical reaction parameter the mass transfer rate is also enhanced. Also, it was detected that the values of Nusselt number is increased and values of heat transfer rate is decreased with the increment of heat absorption parameter.

Table: 2 Mathematical values of $g'(0), \theta'(0)$, Nu and $\zeta'(0)$ for different values of ϕ, M and Ws

ϕ	M	Ws	$g'(0)$	$\theta'(0)$	Nu	$\zeta'(0)$
0.00			-1.801426	0.090608	-0.090608	-1.005397
0.05			-1.732809	0.090722	-0.096181	-1.000985
0.10			-1.667339	0.090849	-0.102008	-0.998823
0.15			-1.604765	0.090994	-0.108108	-0.998698
0.20			-1.544854	0.091156	-0.114503	-1.000448
	0.80		-0.617256	0.092753	-0.104640	-1.014617

1.60		-0.858520	0.091919	-0.103699	-1.008351
2.40		-1.077168	0.091476	-0.103199	-1.004513
3.20		-1.274977	0.091206	-0.102895	-1.002010
4.00		-1.455590	0.091023	-0.102688	-1.000272
	0.20	-2.010126	0.603381	-0.680705	-1.311467
	0.40	-1.916123	0.245684	-0.277169	-1.223771
	0.60	-1.826824	0.155217	-0.175109	-1.142561
	0.80	-1.742155	0.114415	-0.129078	-1.067639
	1.00	-1.662017	0.090861	-0.102505	-0.998737

Table: 3 Mathematical values of $\theta'(0)$, Nu and $\zeta'(0)$ are discussed for different parameter

P_r	γ	Q	$\theta'(0)$	Nu	$\zeta'(0)$
1.0			0.243662	-1.624746	
2.0			0.424746	-1.821571	
3.0			0.493599	-2.187393	
4.0			0.510558	-2.711169	
5.0			0.507469	-3.445510	
	0.08				-0.313578
	0.16				-0.530385
	0.24				-0.707505
	0.32				-0.861141
	0.40				-0.998737
		0.00	-3.330669	-1.624746	
		0.02	0.020191	-1.821571	
		0.04	0.040383	-2.187394	
		0.06	0.060574	-2.711169	
		0.08	0.080766	-3.445510	

From fig (1-5) it is visualized that the profile of radial velocity, tangential velocity, temperature distribution and concentration is increased while the axial velocity is reduced with the enhance of nanoparticle concentration. Physically, greater nanoparticles makes the fluid dense which shortens velocity BL. However, the thermal conductivity of nanofluids is enhanced due to an rise in the volume of nanoparticles. Thus the momentum boundary layer showed a downward trend due to enhanced the thermal conductivity.

Figure 1: *Radial velocity for Nano-particle concentration*

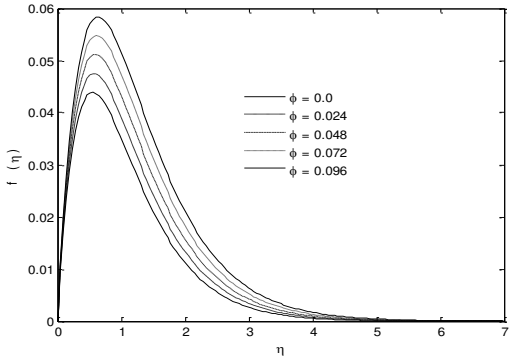

Figure 2: *Axial velocity for Nano-particle concentration*

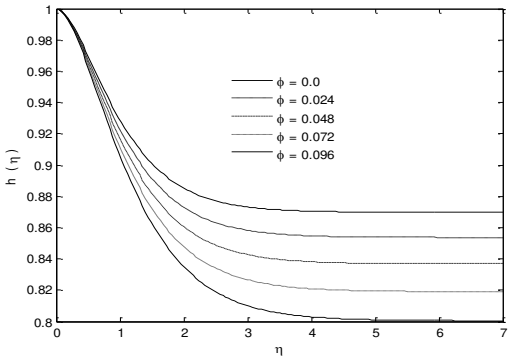

Figure 3: *tangential velocity for Nano-particle concentration*

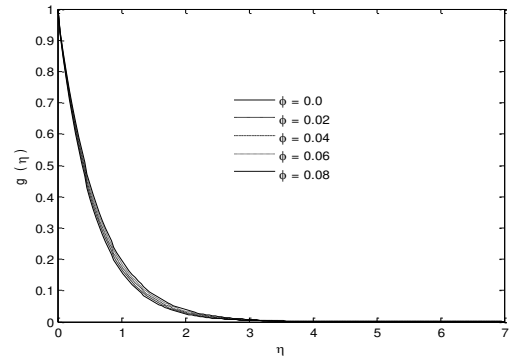

Figure 4: *temperature distribution for Nano-particle concentration*

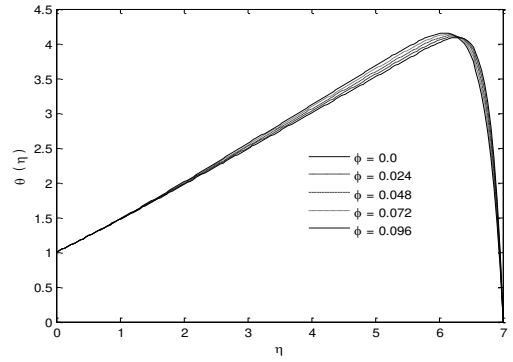

Figure 5: *Concentration profile for Nano-particle concentration*

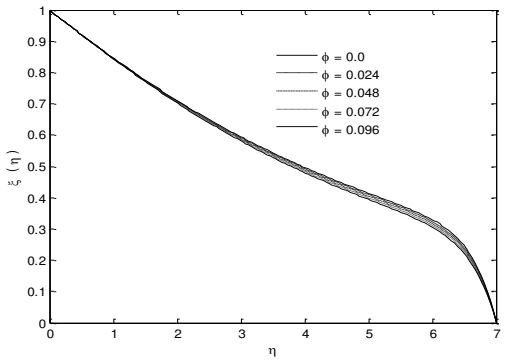

Figure 6: *Radial velocity for Magnetic parameter*

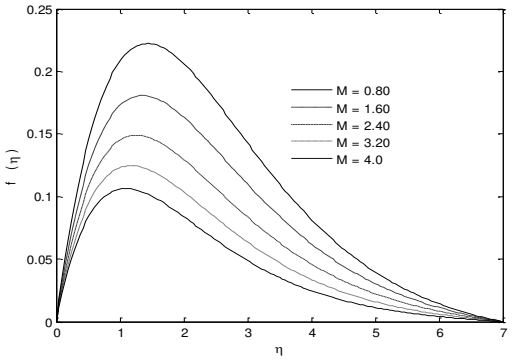

With the increment of volume fraction parameter, the thermal conductivity of fluid is increased therefore the temperature is increased. Fig (6-10) display the impact of Magnetic field parameter over the radial velocity, axial velocity, tangential velocity, temperature distribution profile and concentration profile of the fluid on a rotating porous disk. It was noticed that with the enhancement of magnetic parameter the radial velocity and tangential velocity of the fluid is reduced but the axial velocity, temperature distribution profile and concentration profile of the fluid is enhanced. Due to magnetic field over a fluid which is electrically conducting a Lorentz force is produced. By the increase of temperature at disk, Lorentz force has ability to slow down the fluid motion. So. when the magnetic become greater the thickness of the thermal boundary layer is enhanced, then the velocity profile in axial, tangential and radial direction are reduced. It was observed that over the temperature distribution the effect of magnetic parameter is negligible and in the presence of centrifugal force near to the surface of the disk the radial velocity profile of the fluid is maximum value. Effect of radial velocity, axial velocity, tangential velocity, temperature distribution profile and concentration profile of the fluid for suction parameter is explained in fig (11-15) and observed that the suction parameter has increasing effects on radial velocity, axial

velocity, tangential velocity, temperature and concentration of the fluid over a rotating porous disk. Fig (16) present that for higher values of Prandtl number the expansion behavior is shown in profile of temperature distribution. Prandtl number is defined as the ratio between momentum diffusivity and thermal diffusivity. With the enhancement of Prandtl number the thickness of the thermal boundary is reduced therefore Prandtl number shows his effect over temperature distribution profile. Figure (17) illustrate that the concentration profile is increased, when the Schmidt number is increased. Rate of momentum diffusivity to the mass diffusivity is known as a Schmidt number, momentum diffusivity of the fluid is increased with the enhanced of Schmidt number therefore concentration profile is enhanced. It is cleared from fig (18) when the heat absorption/ heat generation parameter is enhanced the temperature distribution profile is also enhanced. Actually, heat absorption decreases the thermal boundary layer thickness but heat generation enhanced the thickness of thermal boundary layer. With the increment of heat absorption shows that heat is reserved from a system by any source. Therefore, thickness of thermal boundary layer is decreased with the increase of heat absorption and rate of heat transfer is also increased from Table (2). Fig (19) describe that for larger values of chemical reaction parameter shows the decline behavior in profile of concentration. With the enhancement of chemical reaction parameter resemble to the higher amount of destructive chemical reaction which can diffuse liquid specie more efficiently.

Figure 7: *Radial velocity for Magnetic parameter*

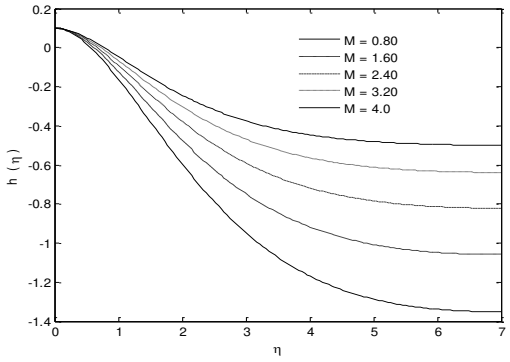

Figure 8: *Tangential velocity for Magnetic parameter*

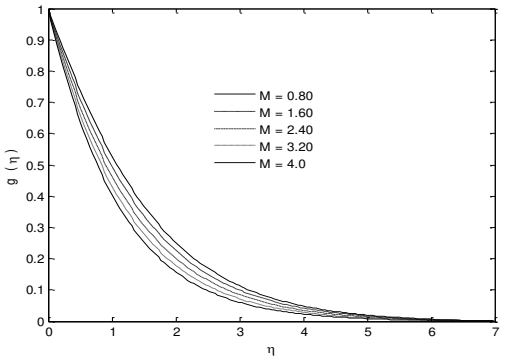

Figure 9: *Temperature distribution profile for Magnetic parameter*

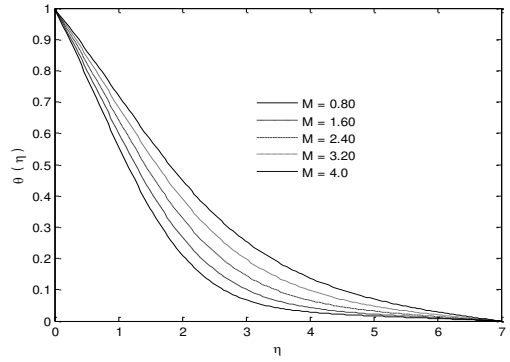

Figure 10: *Concentration profile for Magnetic parameter*

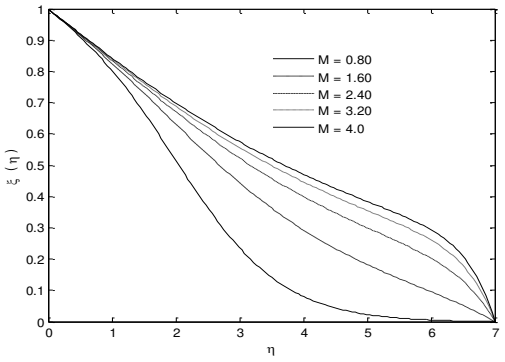

Figure 11: *Temperature distribution profile for Prandtl number*

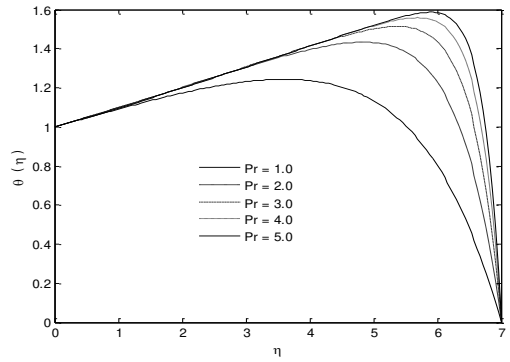

Figure 12: *radial velocity for Suction parameter*

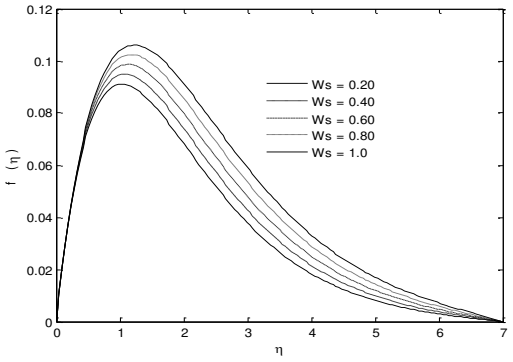

Figure 13: *Axial velocity for Suction parameter*

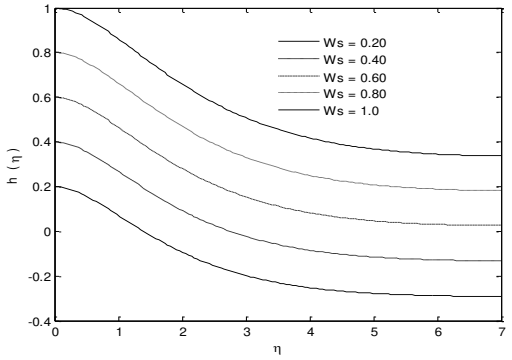

Figure 14: *Tangential velocity for Suction parameter*

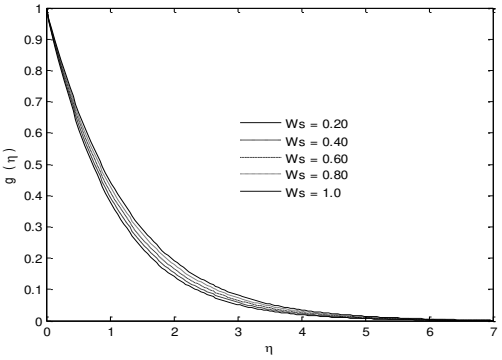

Figure 15: *Temperature distribution for Suction parameter*

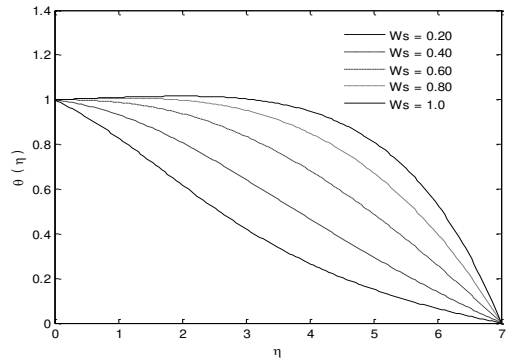

Figure 16: *Concentration profile for Suction parameter*

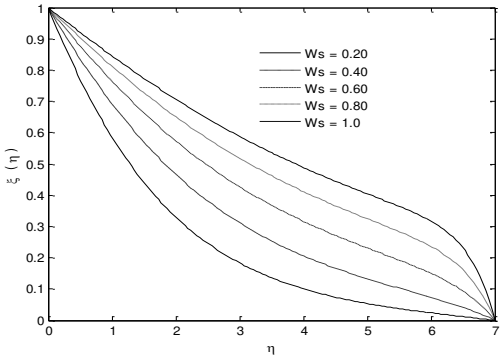

Figure 17: *Concentration profile for Schmidt number*

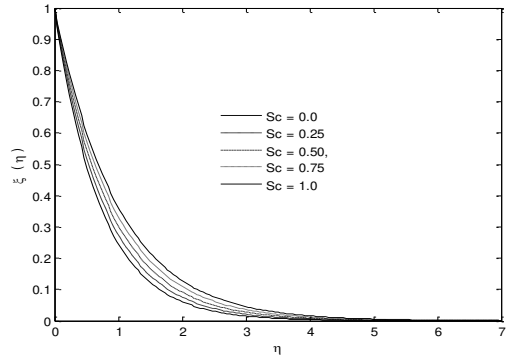

Figure 18: *Temperature distribution profile for heat generation/absorption*

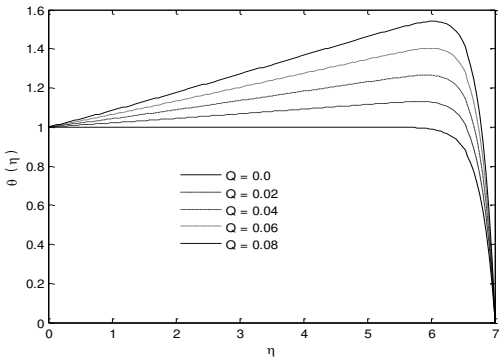

Figure 19: *Concentration profile for chemical reaction parameter*

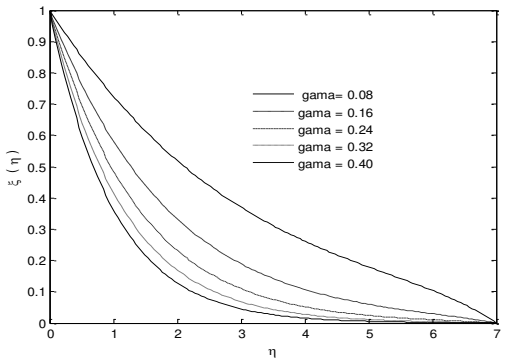

Conclusion:

A numerical study of nanofluid flow over the rotating disk with the existence of a magnetic parameter with chemical reaction was analyzed here. The finite difference method was employed to obtain the results of their model numerically. Significance of the influence of various physical parameter under discussion on the non-dimensional concentration, velocity, and temperature profiles are delineated graphically. The skin friction coefficient and the Nusselt number for various values of the different governing parameters are listed in tabular form. After a thorough investigation, we have reached the following concluding observation:

- Nusselt number is increased but the heat transfer rate is decreased with the increment of heat source parameter.
- Concentration distribution is enhancing for the Schmidt number and chemical reaction parameter.
- For higher values of nanoparticle concentration and Prandtl number, the heat and mass transfer are increased but opposite behavior is seen for the magnetic and suction parameter.
- Shear stress and Nusselt number have a decreasing effect for suction parameter and nanoparticle concentration. But for the magnetic parameter shear stress of the fluid is enhanced.

- Increasing behavior of axial velocity, tangential velocity, and concentration of the fluid was noticed on the magnetic parameter.
- The suction parameter has the same effect for radial velocity, tangential velocity, axial velocity, temperature, and concentration of a fluid.
- Fluid Temperature is increased with the enhancement of heat absorption and Prandtl number.
- It was observed that with the expansion of nanoparticle concentration radial velocity, tangential velocity and temperature of the fluid was enhanced but reverse reaction for axial velocity.

Acknowledgments:

The authors acknowledge the financial support provided by the Center of Excellence in Theoretical and Computational Science (TaCS-CoE), KMUTT.

Moreover, this research project is supported by Thailand Science Research and Innovation (TSRI) Basic Research Fund: Fiscal year 2021 under project number 64A306000005.

Conflict of Interest: The authors declare that there is no conflict of interest.

Authors contribution:

Conceptualization: M. Ramzan, P. Kumam, K.S Nisar; **Writing - original draft**: M. Ramzan, K.S. Nisar and I. Khan; **Investigation**: P. Kumam, K.S. Nisar, I. Khan and W. Jamshed; **Data curation**: M.Ramzan, K.S. Nisar and W. Jamshed; **Formal analysis**: P. Kumam, M. Ramzan, and I. Khan; **Software**: M. Ramzan, K.S. Nisar and W. Jamshed; **Supervision**: P. Kumam, K.S. Nisar and I. Khan; **Writing - review editing**: P. Kumam, K.S Nisar and W. Jamshed

References:

[1] B. Mahanthesh, B. J. Gireesha, S. A. Shahzad, A. Rauf and P. B. S. Kumar, Nonlinear radiated MHD flow of nanofluids due to a rotating disk with irregular heat source and heat flux condition, “Results in Physics”. vol. 7, pp. 2375-2383, 2017.

[2] Hayat T, Rashid M, Imtiaz M, Alsaedi, A. Magnetohydrodynamic (MHD) flow of Cu-water nanofluid due to a rotating disk with partial slip. “AIP Advances”, vol. 5, pp. 067169, 2015.

[3] C. Yin, L. Zheng, C. Zhang and X. Zhang, Flow and heat transfer of nanofluids over a rotating disk with uniform stretching rate in the radial direction, “Propulsion Power Research”, vol. 6, pp. 25-30, 2017.

[4] T. Hayat, T. Muhammad, S. A. Shehzad and A. Alsaedi, On magnetohydrodynamic flow of nanofluid due to a rotating disk with slip effect: A numerical study, “Computer Methods in Applied Mechanics and Engineering”, vol. 315, pp. 467-477, 2017.

[5] M. Imtiaz, T. Hayat, A. Alsaedi, S. Asghar, Slip flow by a variable thickness rotating disk subject to magnetohydrodynamics, “Results in Physics”, Vol. 7, pp. 503-309, 2017.

[6] M. M. Rashidi, S. Abelman and N. Freidoonimehr, Entropy generation in steady MHD flow due to a rotating porous disk in a nanofluid, “International Journal of Heat and Mass Transfer”, vol. 62, pp. 515-525, 2013.

[7] M. Mustafa, M. MHD nanofluid flow over a rotating disk with partial slip effects: Buongiorno model, “International Journal of Heat and Mass Transfer”, vol. 108, pp. 1910-1916, 2017.

[8] M. Turkyilmazoglu, Nanofluid flow and heat transfer due to a rotating disk, “Computers & Fluids”, vol. 94, pp. 139–146, 2014.

[9] Y. Lin and L. Zheng, Marangoni boundary layer flow and heat transfer of copper-water nanofluid over a porous medium disk, “AIP- Advances”, vol. 134(4), pp.1-7 (2012).

[10] M. Sheikholeslami, M. Hatami, D. D. Ganji, Numerical investigation of nanofluid spraying on an inclined rotating disk for cooling process, “Journal of Molecular Liquids”, vol. 211, pp. 577-583, 2015.

[11] M. Turkyilmazoglu and P. Senel, Heat and mass transfer of the flow due to a rotating rough and porous disk, “International Journal of Thermal Sciences”, vol. 63, pp. 146–158, 2013

[12] S. P. A. Devi and R. U. Devi, On hydromagnetic flow due to a rotating disk with radiation effects. “Nonlinear Analysis: Modelling and Control”, vol. 16(1), pp. 17–29, 2011.

[13] E. Osalusi, Effects of thermal radiation on MHD and slip flow over a porous rotating disk with variable properties, “Romanian Journal of Physics RJP”, Vol. 52(3–4), pp. 217–229, 2007.

[14] N. A. Khan, S. Aziz and N. A. Khan, Numerical Simulation for the Unsteady MHD Flow and Heat Transfer of Couple Stress Fluid over a Rotating Disk. “Plos One,” vol. 9(5), 2014

[15] A. Arikoglu, I. Ozkol, On the MHD and slip flow over a rotating disk with heat transfer, “International Journal of Numerical Methods for Heat and FLuid Flow”, vol. 28(2), pp. 172-184, 2006.

[16] S. Nadeem and S. Saleem, Analytical study of third grade fluid over a rotating vertical cone in the presence of nanoparticles, “International Journal of Heat and Mass Transfer”, vol. 85, pp. 1041-1048, 2015.

[17] A. Hafeez, M. Khan and J. Ahmed, Stagnation point flow of radiative Oldroyd-B nanofluid over a rotating disk, “Computer Methods and Programs in Biomedicine”, vol. 191, pp. 105-342, 2020.

[18] A. Abbasi. F. Mabood, W. Farooq and M. Batool, Bioconvective flow of viscoelastic Nanofluid over a convective rotating stretching disk, “International Journal of Heat and Mass Transfer”, vol. 119, pp. 104921, 2020.

[19] F. Ali, M. Saqib, I. Khan & N. A. Sheikh Application of Caputo-Fabrizio derivatives to MHD free convection flow of generalized Walters'-B fluid model. "The European Physical Journal Plus", vol. 131(10), pp. 377, 2016.

[20] M. Saqib, H. Hanif, T. Abdeljawad, I. Khan, S. Shafie and K. S. Nisar, Heat Transfer in MHD Flow of Maxwell Fluid via Fractional Cattaneo-Friedrich Model: A Finite Difference Approach, "Cmc-Computers Materials & Continua", vol. 65(3), pp. 1959-1973, 2020.

[21] M. Saqib, I. Khan, Y. M. Chu, A. Qushairi, S. Shafie and K. S. Nisar, Multiple Fractional Solutions for Magnetic Bio-Nanofluid Using Oldroyd-B Model in a Porous Medium with Ramped Wall Heating and Variable Velocity, "Applied Science", vol. 10(11), pp. 3886, 2020.

[22] M. Saqib, A. R. M. Kasim, N. F. Mohammad, D. L.C. Ching and S. Shafie, Application of Fractional Derivative Without Singular and Local Kernel to Enhanced Heat Transfer in CNTs Nanofluid Over an Inclined Plate, "Symmetry", vol. 12(5), pp. 768, 2020.

[23] M. Saqib, S. Shafie, I. Khan, Y. M. chu and K. S. Nisar, Symmetric MHD Channel Flow of Nonlocal Fractional Model of BTF Containing Hybrid Nanoparticles. "Symmetry", vol. 12(4), pp. 663, 2020.

[24] I. Khan, M. Saqib and A. M. Alqahtani, Channel flow of fractionalized H2O-based CNTs nanofluids with Newtonian heating, “Discrete & Continuous Dynamical Systems-S”, vol. 13(3), pp. 769, 2018.

[25] I. Khan, M. Saqib and F. Ali, Application of time-fractional derivatives with non-singular kernel to the generalized convective flow of Casson fluid in a microchannel with constant walls temperature. “The European Physical Journal Special Topics”, vol. 226(16-18), pp. 3791-3802, 2017 .

[26] M. Saqib, I. Khan and S. Shafie, Generalized magnetic blood flow in a cylindrical tube with magnetite dusty particles, “Journal of Magnetism and Magnetic Materials”, vol. 484, 490-496, 2019.

[27] F. M. Oudina, A. Aissa, B. Mahanthesh and H. F. Öztop, Heat transport of magnetized Newtonian nanoliquids in an annular space between porous vertical cylinders with discrete heat source, International Communications in Heat and Mass Transfer, vol. 117, pp. 104737, 2020.

[28] F. M. Oudina , Convective heat transfer of Titania nanofluids of different base fluids in cylindrical annulus with discrete heat source, “Heat Transfer-Asian Research”, pp. 1-13, 2018.

[29] S. Marzougui, F. M.Oudina, A. Assia, M. Magherbi, Z. Shah and K. Ramesh, Entropy generation on magneto-convective flow of copper–water nanofluid in a cavity with chamfers, “Journal of Thermal Analysis and Calorimetry”, 2020

[30] U. Khan, A. Zaib and F. M.Oudina, Mixed Convective Magneto Flow of SiO2–MoS2/C2H6O2 Hybrid Nanoliquids Through a Vertical Stretching/Shrinking Wedge:

Stability Analysis, “Arabian Journal for Science and Engineering”, 45, pp. 9061-9073, 2020.

[31] F. M. Oudina, N. K. Reddy and M. Sankar, Heat Source Location Effects on Buoyant Convection of Nanofluids in an Annulus, “Advances in Fluid Dynamics”, pp. 923-937, 2020.

[32] A. Ishak, R. Nazar and I. Pop, Mixed convection on the stagnation point flow towards a vertical, continuously stretching sheet. ASME, Journal of Heat Transfer, vol. 129, pp 1087–1090, 2007.

[33] A. Ishak, R. Nazar and I. Pop, Boundary layer flow and heat transfer over an unsteady stretching vertical surface. Meccanica, vol. 44, pp 369–375, 2009.

[34] M. H. Abolbashari, N. Freidoonimehr, F. Nazari and M. M. Rashidi, Entropy analysis for an unsteady MHD flow past a stretching permeable surface in nano-fluid. Powder Technology, vol. 267, pp 256–267, 2014.

[35] S. Das, S. Chakraborty, R. N. Jana, and O. D. Makinde, Entropy analysis of unsteady magneto-nanofluid flow past accelerating stretching sheet with convective boundary condition, Applied Mathematics and Mechanics, vol. 36(2), pp 1593–1610, 2015

[36] W. Jamshed, V. Kumar and V. Kumar, “Computational examination of Casson nanofluid due to a non-linear stretching sheet subjected to particle shape factor: Tiwari and Das model, “Numerical Methods for Partial Differential Equations”, 2020.

[37] W. Jamshed, “Numerical Investigation of MHD Impact on Maxwell Nanofluid, “International Communications in Heat and Mass Transfer”, 2020.

Figures

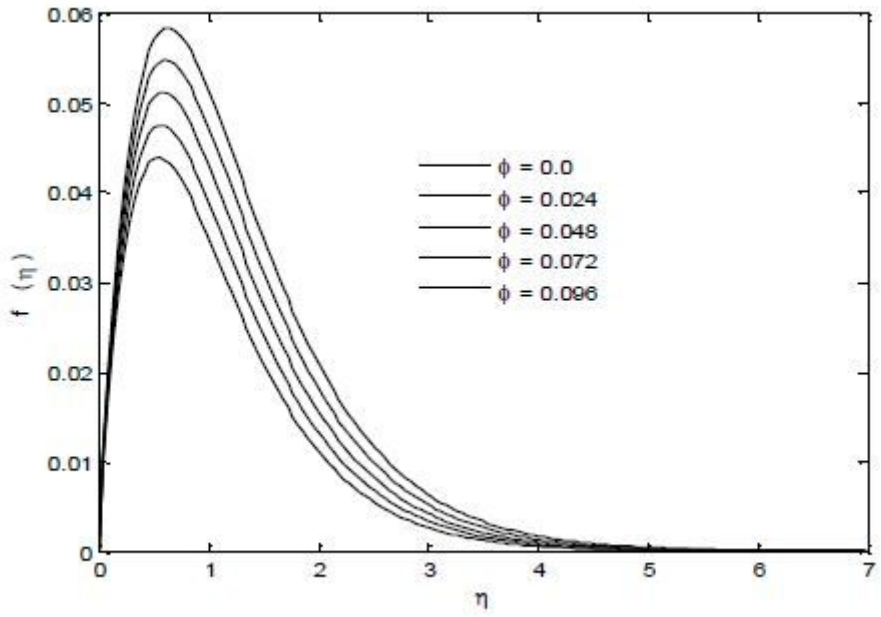

Figure 1

Radial velocity for Nano-particle concentration

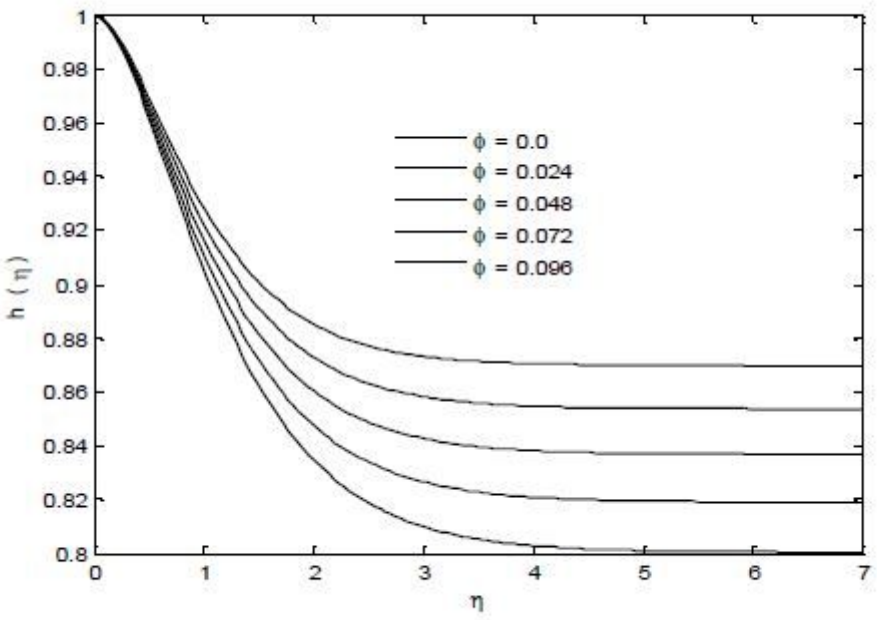

Figure 2

Axial velocity for Nano-particle concentration

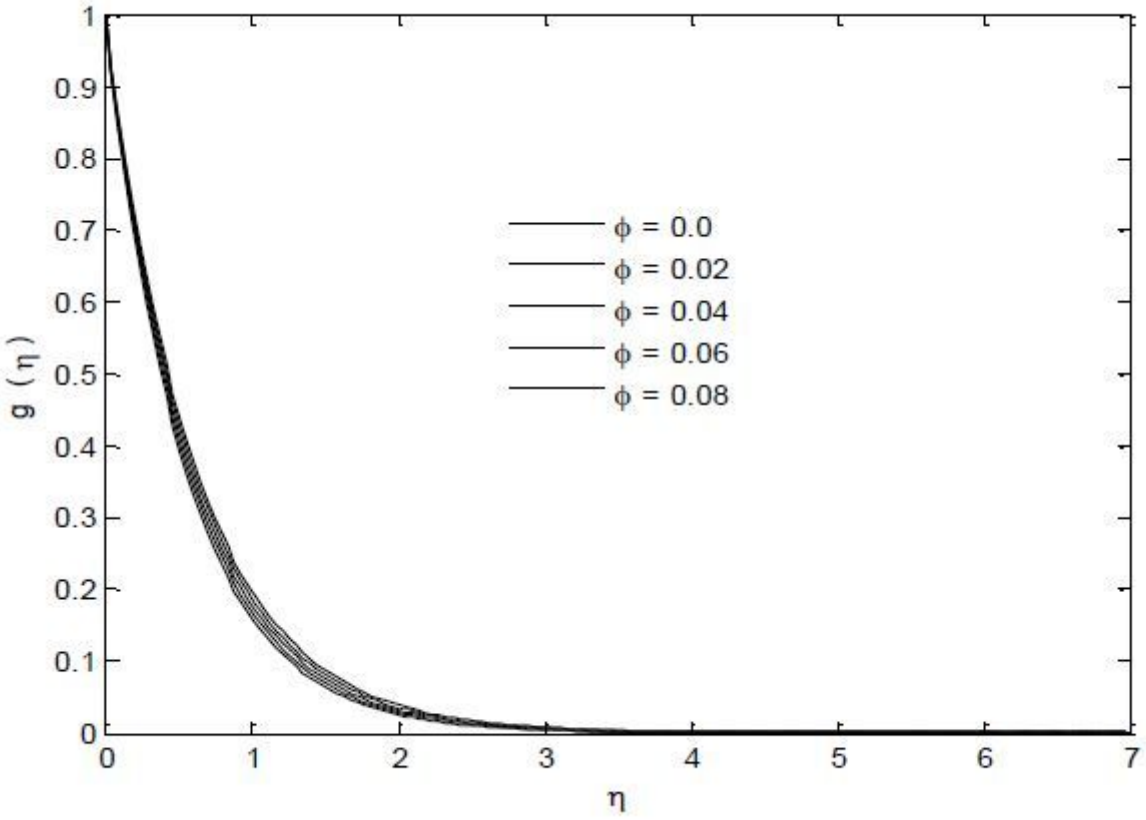

Figure 3

tangential velocity for Nano-particle concentration

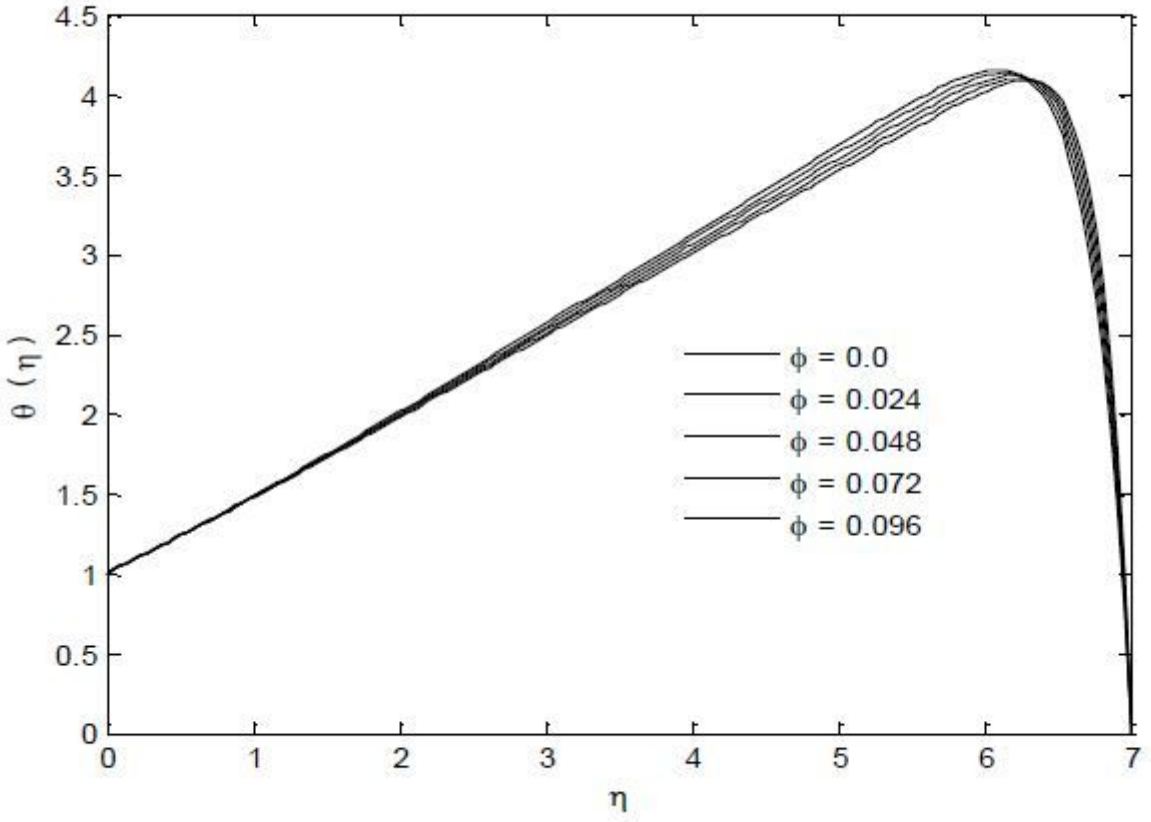

Figure 4

temperature distribution for Nano-particle concentration

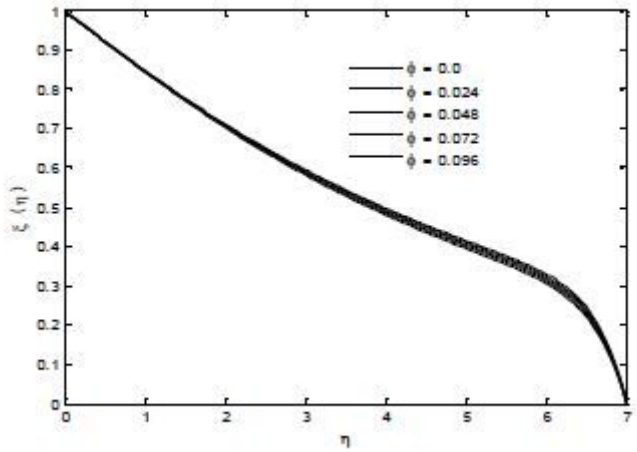

Figure 5

Concentration profile for Nano-particle concentration

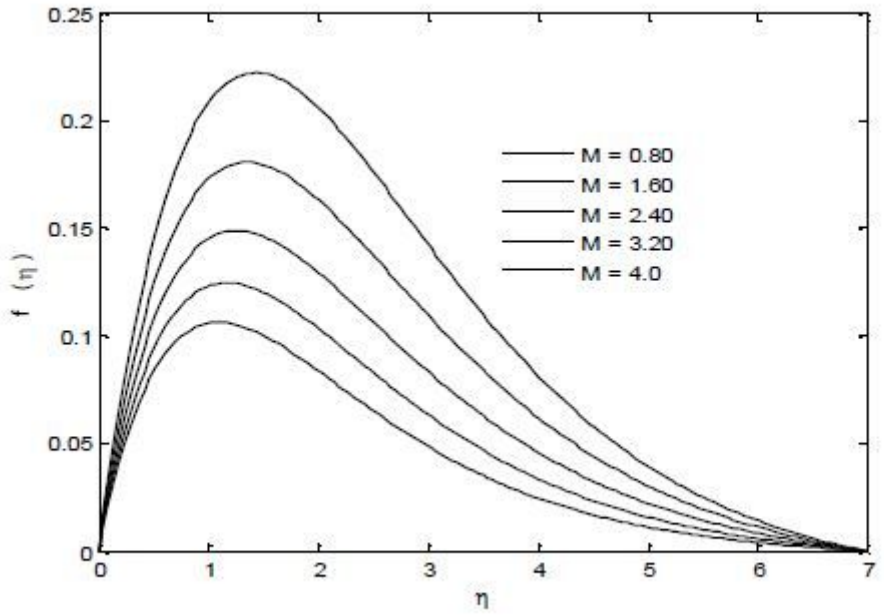

Figure 6

Radial velocity for Magnetic parameter

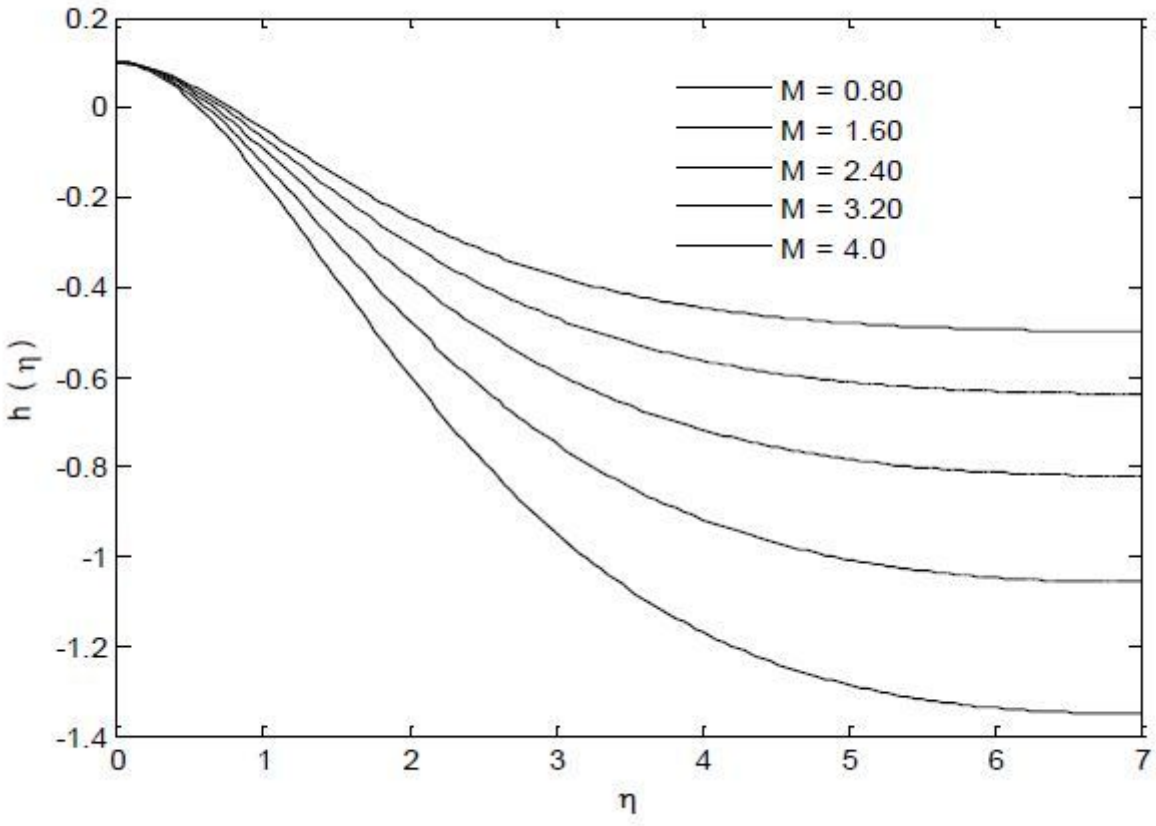

Figure 7

Radial velocity for Magnetic parameter

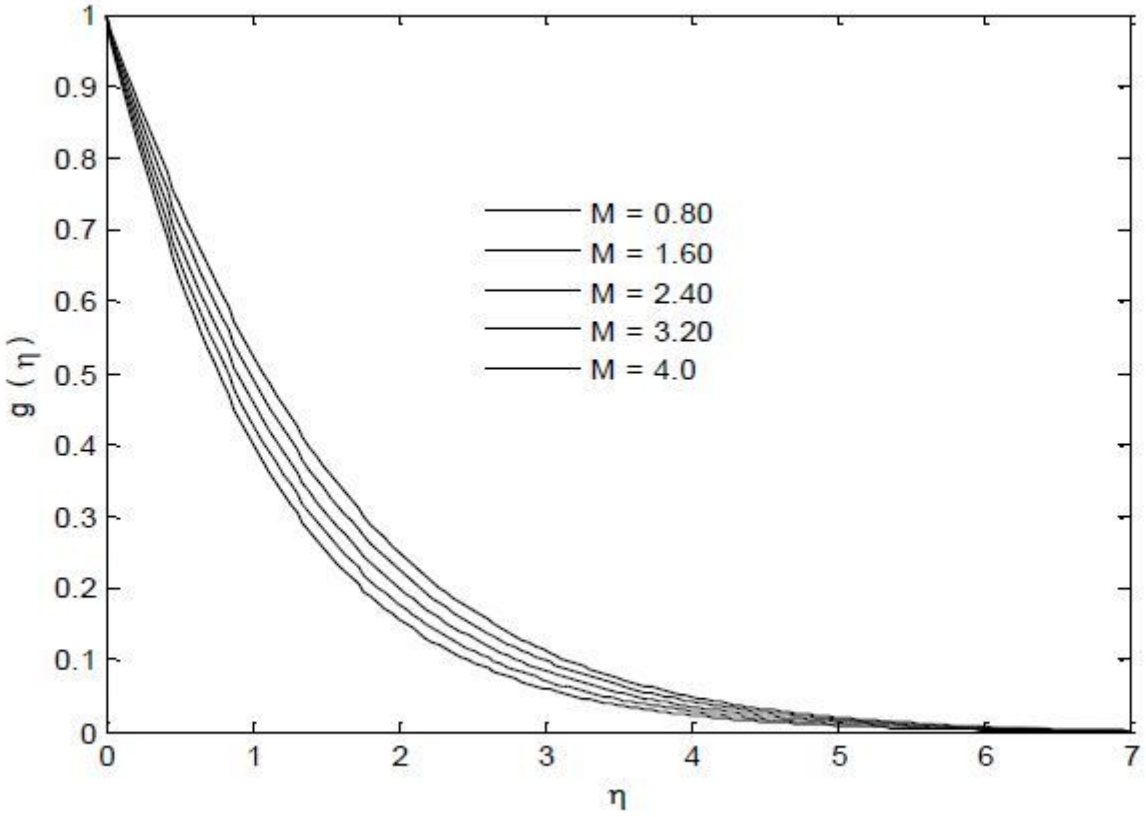

Figure 8

Tangential velocity for Magnetic parameter

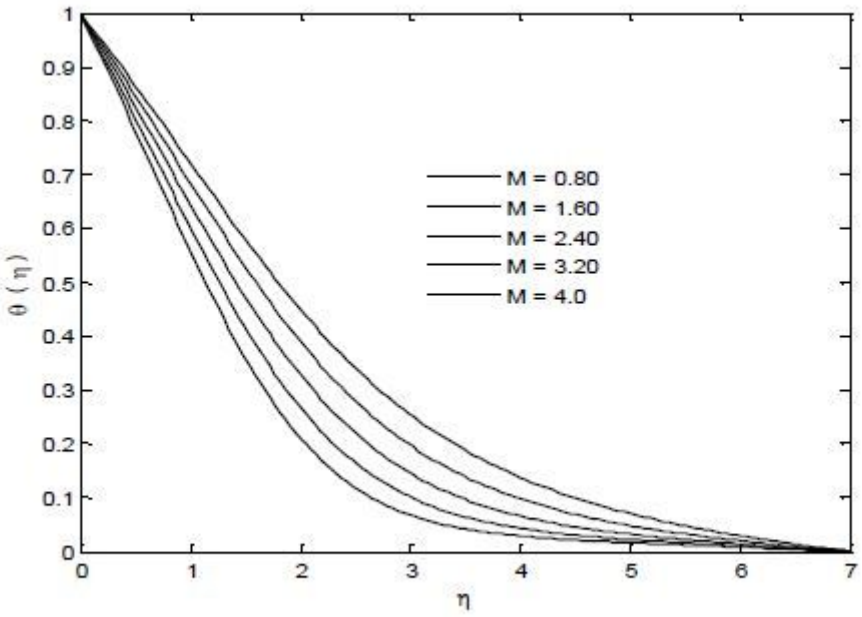

Figure 9

Temperature distribution profile for Magnetic parameter

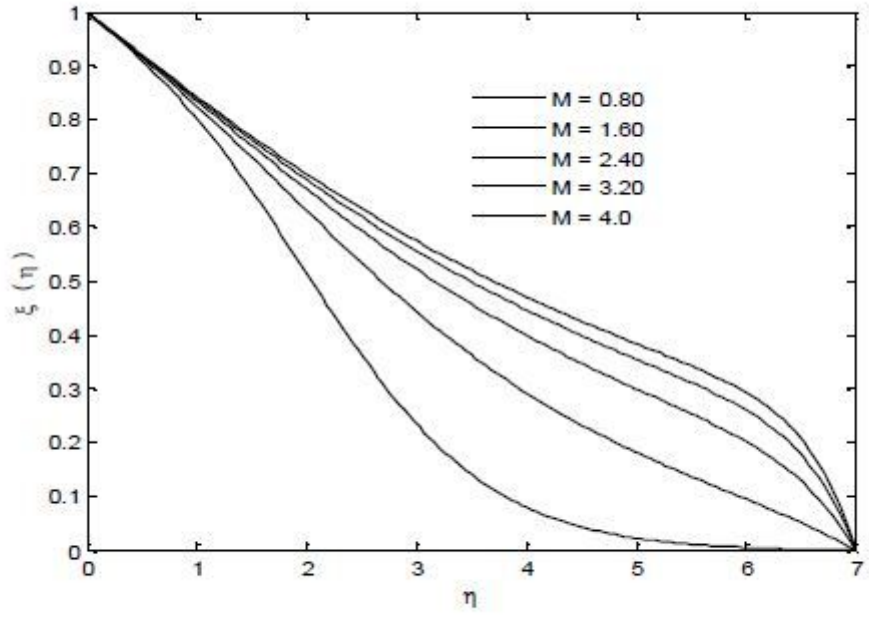

Figure 10

Concentration profile for Magnetic parameter

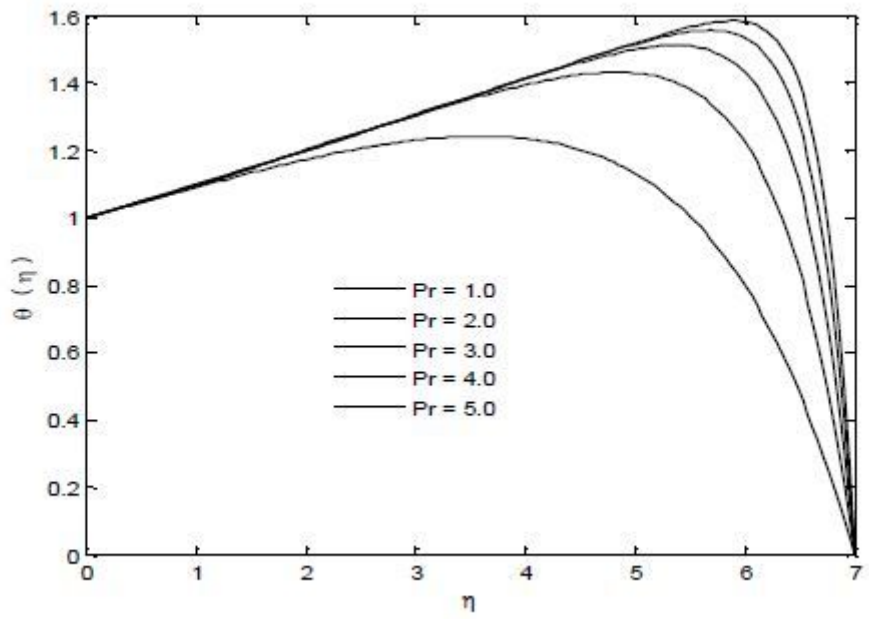

Figure 11

Temperature distribution profile for Prandtl number

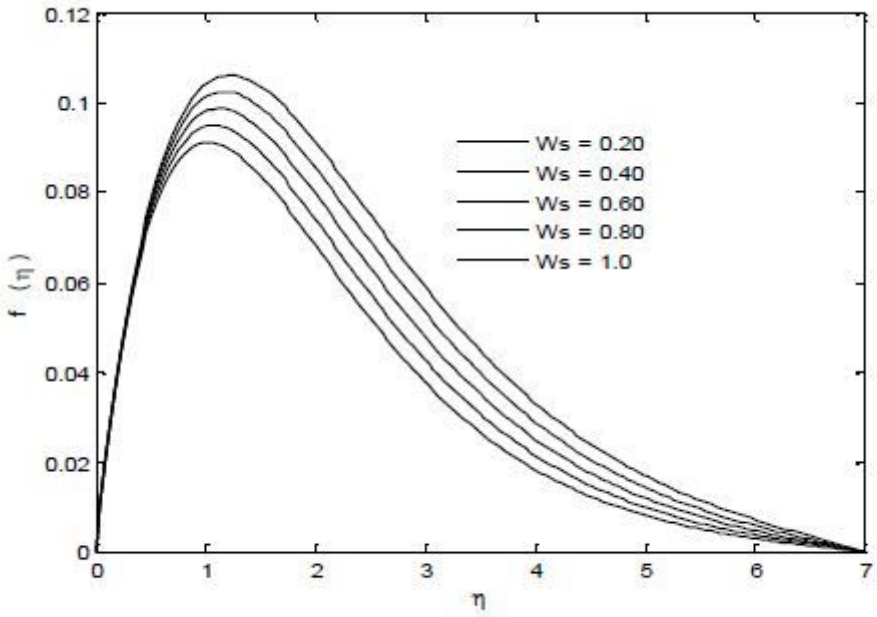

Figure 12

radial velocity for Suction parameter

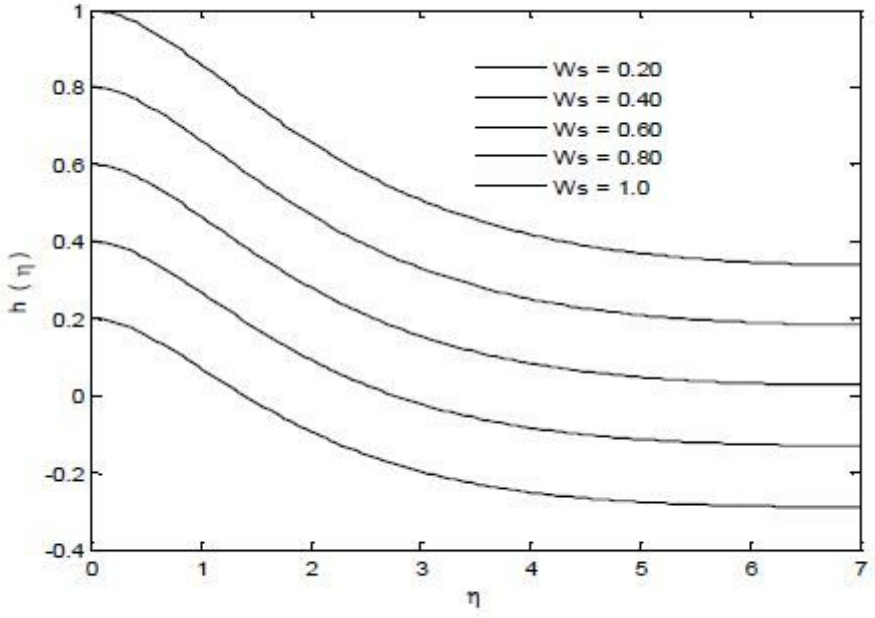

Figure 13

Axial velocity for Suction parameter

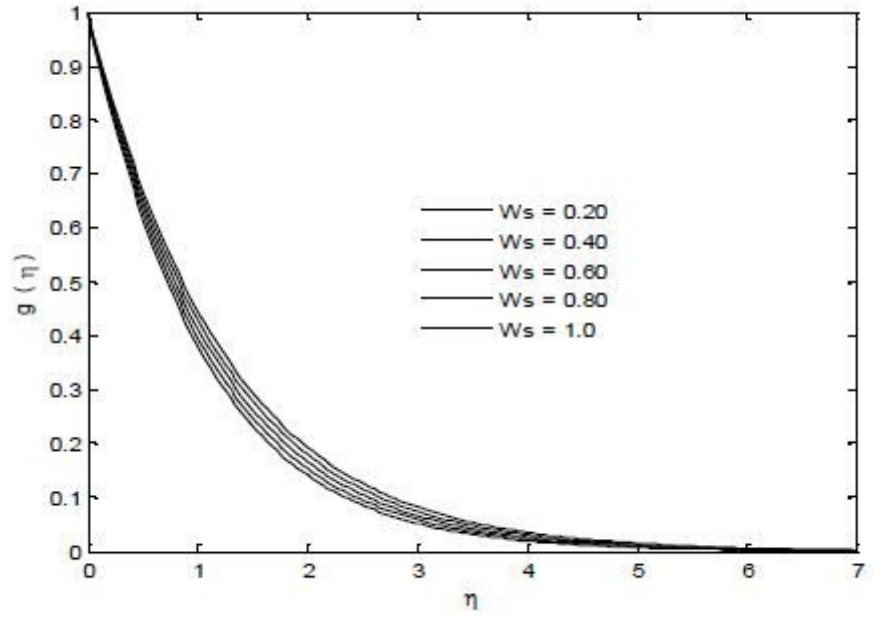

Figure 14

Tangential velocity for Suction parameter

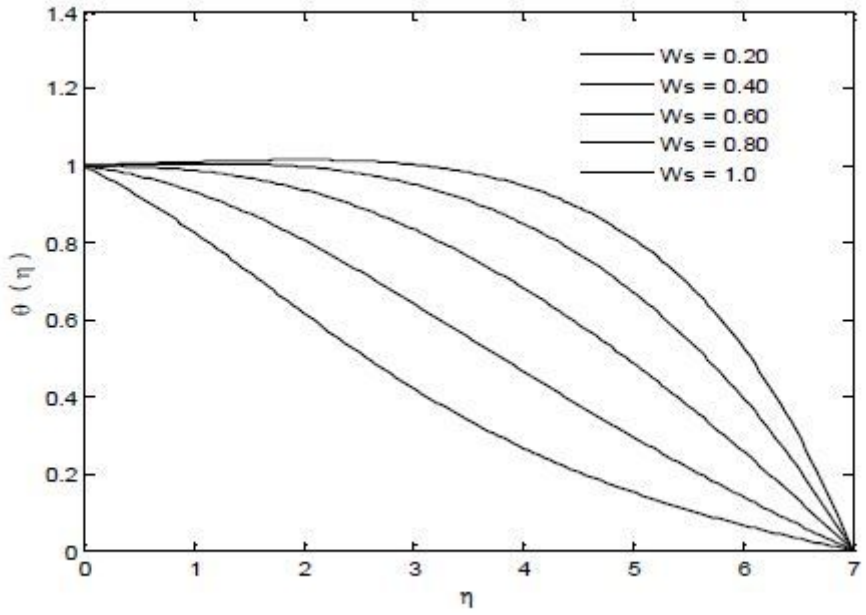

Figure 15

Temperature distribution for Suction parameter

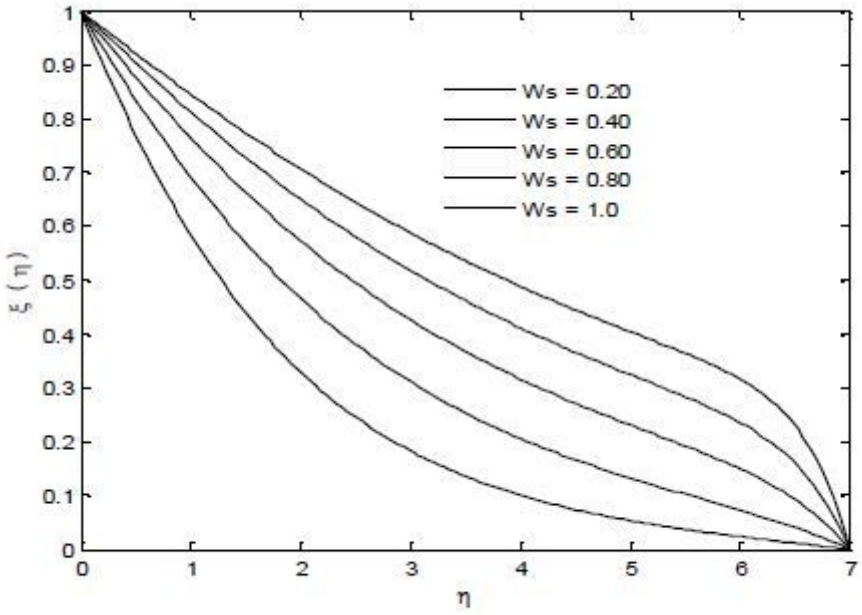

Figure 16

Concentration profile for Suction parameter

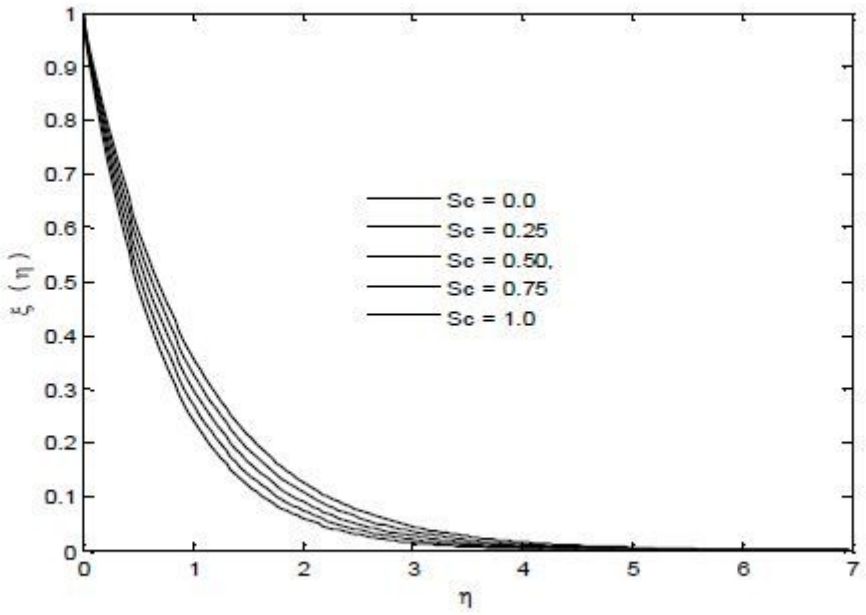

Figure 17

Concentration profile for Schmidt number

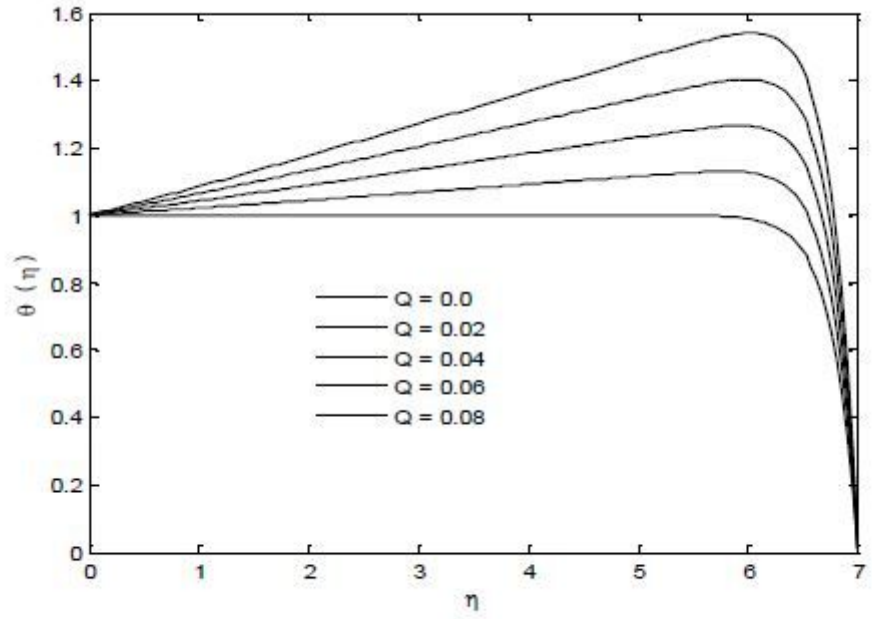

Figure 18

Temperatur

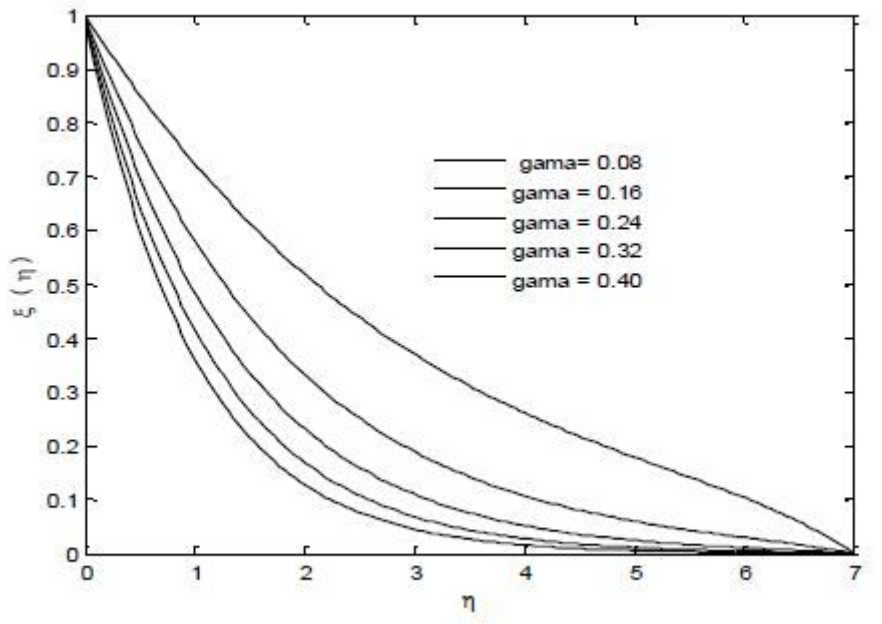

Figure 19

Concentration profile for chemical reaction parameter

Supplementary Files

This is a list of supplementary files associated with this preprint. Click to download.

- FigA.jpg